Postprint of: Meller M., Stawiarski K., On Radar DoA Estimation and Tilted Rotating Electronically Scanned Arrays (2020), 21st International Radar Symposium (IRS), 05-08.10.2020, Warsaw, Poland, DOI: 10.23919/IRS48640.2020.9253871

On Radar DoA Estimation and Tilted Rotating Electronically Scanned Arrays

Michał Meller*,† and Kamil Stawiarski*,†
* Gdańsk University of Technology, Faculty of Electronics, Telecommunications and Computer Science,
Department of Automatic Control, ul. Narutowicza 11/12, 80-233 Gdańsk, POLAND
† PIT-RADWAR S.A., ul. Poligonowa 30, 04-051 Warsaw, POLAND
Corresponding author e-mail: michal.meller@pitradwar.com

***Abstract*—We consider DoA estimation in a monopulse radar system employing a tilted rotating array. We investigate the case of nonzero steering angles, in which case the mapping between the target's azimuth and elevation in the global coordinate system and their counterparts in the array local coordinate system becomes increasingly nonlinear and coupled. Since estimating the azimuth using coherently integrated signals might be difficult because of strong modulation in the difference signal induced by the rotation of the antenna, we develop an iterative approach that alternates between estimating the elevation using coherently integrated signals and estimating the azimuth using unfiltered signals. We also develop a simplified version of the scheme, which employs only one iteration and forms the final estimates by applying simple corrections to results of the first iteration.**

***Index Terms*—direction of arrival, estimation, radar**

I. Introduction

In applications where very high update rates are not needed, but full azimuth coverage is required, radars employing a rotating array are usually preferred over considerably more costly systems that employ multiple stationary (fixed) arrays. Owing to the progress in the active electronic scan array (AESA) and digital beamforming (DBF) technologies, such radars can nearly simultaneously perform multiple functions, among others the volume and the horizon scan, tracking, or the classification of non-cooperative targets, all within tightly restricted time budget imposed by the rotation of the array [1].

A somewhat overlooked disadvantage of using a rotating electronically scanned array is that accurate estimation of target azimuth and elevation coordinates becomes more difficult than with a fixed array. This increased difficulty stems from several reasons, which we will explain here briefly. To detect targets, a radar emits a trail of pulses and processes the returning echo. The processing typically includes some form of coherent integration (Doppler filtering) whose aim is to improve the signal to noise ration and to reject clutter. Ideally, the signal that is integrated should be stationary, which is difficult to satisfy with a rotating array. Consider as an example a so-called monopulse system, which is a classical method employed by radar engineers to solve the target angle estimation problem [2]. In this approach, to estimate one angle two beams, called sum and difference (or sigma and delta), are required. The sum beam has typical beampattern with a narrow mainlobe and a number of low sidelobes, while the difference beam has a sharp null at the peak of the sum beam. The rotation of the array results in modulation of the azimuth difference signal, which might cause estimation bias if coherent integration is employed prior to the monopulse. In this situation one might attempt to estimate the azimuth angle using by applying the monopulse to each echo pulse separately and averaging the partial estimates. Such approach, however, is well known to be considerably suboptimal due to poor behavior of the monopulse at low signal to noise ratios. More sophisticated approaches, that process all echo pulses jointly, were proposed in, e.g., [3], [4]. Even though the authors employed the maximum likelihood (ML) approach in both cases, the schemes differ because of different assumptions made. The scheme from [3] assumes a coherent system and a nonfluctuating target, which leads to the so-called deterministic ML estimator, while the scheme from [4] makes no assumption on the coherence and assumes a fluctuating target, which results in the stochastic ML estimator [5].

The second difficulty in estimating the angular coordinates is the consequence of the electronic scan capability. Steering a beam causes a distortion of the array beampattern that increases with the beam steering angles. The mainlobe of the beampattern widens, and the entire beampattern flexes in a "banana-like" shape (see Fig. 1), which means that the problems of estimating the azimuth and elevation coordinates can no longer be treated as separate – for example, since the azimuth angle of the center of the beam is a function of the elevation, any error in estimating the elevation will affect the azimuth as well. Note that the deformation of the beampattern that occurs for high steering angles exacerbates when the array is tilted backwards, which is commonly done to improve the array coverage.

With a fixed array, these deformations are not a difficult issue. It is well known that if a beampattern is represented in the uv coordinates, steering has no impact on its shape, apart from shifting the peak of the beam. One may therefore estimate the u and v coordinates of a target separately and convert them to the azimuth and elevation. However, when the array rotates the u and v coordinates of the target change continuously in a nontrivial way, and for best results one should take this effect into account in the estimation process.

Our paper contributes in the following areas: 1. We describe the motion of a target in the coordinate system local to the array that is induced by the rotation of the array. 2. We propose

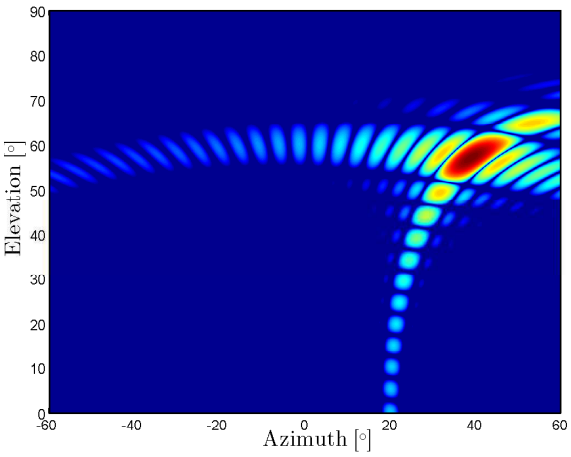

Figure 1. An example of beampattern deformations that occur for high steering angles with an array tilted backwards.

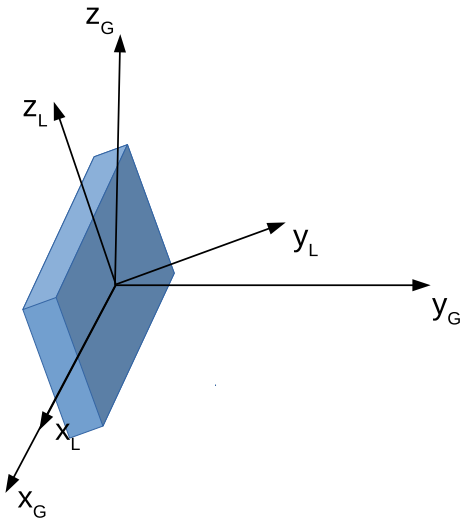

Figure 2. The definition of the local and the global coordinate systems.

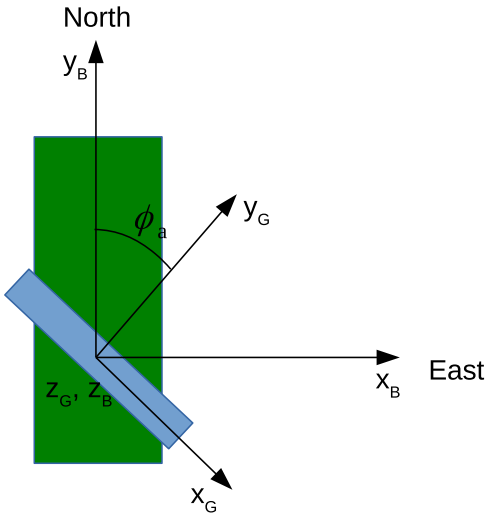

Figure 3. The relation between the base-frame and the array global coordinate systems.

a computationally attractive estimator of azimuth and elevation that is designed to avoid excessive performance degradation at high steering angles. 3. We investigate the proposed method's performance using computer simulations.

The organization of the manuscript follows the pattern set by its contributions. Sections II and III develop the formulas that describe the target motion in the coordinate system local to the array. Section IV contains the description of the proposed approach. Section V presents results of computer simulations. Section VI concludes.

II. Definitions of coordinate systems

Consider a planar array tilted backwards by an angle P. We introduce two array coordinate systems, shown in Fig. 2. The X and Z axes of the array local coordinate system (LCS) match the array face, that is, this system neglects the tilt of the array. The LCS represents how the array "sees" the world around it. It is also the system that is used often by array engineers for array design and measurements. The array global system is obtained from the local array system by rotation about the X axis by an angle $-P$.

Let us also introduce the base-frame coordinate system, which corresponds to the East-North-Up (ENU) system of a radar. The relation between the base frame and the array global coordinate system corresponds to the straightforward rotation about the Z axis by ϕ_{a} – see Fig. 3.

The relation between the azimuth and elevation angles (A, E) and the Cartesian coordinates (X, Y, Z) is given by

$$\begin{aligned} X &= R \sin A \cos E \\ Y &= R \cos A \cos E \\ Z &= R \sin E \end{aligned} \tag{1}$$

where R denotes the range and A, E, X, Y, and Z are all assumed to be in the same coordinate system (e.g. LCS or GCS). To obtain the uv coordinates, set

$$\begin{aligned} u &= \sin A \cos E \\ v &= \sin E \end{aligned} \tag{2}$$

Then

$$\begin{aligned} X &= Ru \\ Y &= Rw \\ Z &= Rv \end{aligned} \tag{3}$$

where $w = \sqrt{1 - u^2 - v^2} = \cos A \cos E$.

We also introduce the (α, E) coordinate system, which is a counterpart of the uv system in which the angles are expressed in degrees (or radians), rather than millisines, which might be preferable when one is not used to the (u, v)

system. The angles in the (α, E) have simple interpretation of specifying two perpendicular cones whose intersection is the point of interest and are related to the (u, v) coordinates in the following way

$$\begin{aligned} u &= \sin\alpha \\ v &= \sin E \end{aligned} \tag{4}$$

Note that, when $E = 0$, it holds that $\alpha = A$.

III. Description of the target motion in the LCS

Using (1)-(4) and the rotation matrix that transforms the GCS to the LCS, one may obtain the transformation between the azimuth and the elevation in the GCS (denoted A_{G} and E_{G}, respectively) and their counterparts in the LCS

$$\begin{aligned} E_{\mathrm{L}} &= \arcsin\left[-\cos A_{\mathrm{G}}\cos E_{\mathrm{G}}\sin P + \sin E_{\mathrm{G}}\cos P\right] \\ A_{\mathrm{L}} &= \arcsin\left[\sin A_{\mathrm{G}}\frac{\cos E_{\mathrm{G}}}{\cos E_L}\right] \end{aligned} \tag{5}$$

The transformation between the $(A_{\mathrm{G}}, E_{\mathrm{G}})$ and the $(\alpha_{\mathrm{L}}, E_{\mathrm{L}})$ coordinates can be obtained in a similar way. It reads

$$\begin{aligned} E_{\mathrm{L}} &= \arcsin\left[-\cos A_{\mathrm{G}}\cos E_{\mathrm{G}}\sin P + \sin E_{\mathrm{G}}\cos P\right] \\ \alpha_{\mathrm{L}} &= \arcsin\left[\sin A_{\mathrm{G}}\cos E_{\mathrm{G}}\right] \end{aligned} \tag{6}$$

Finally, in Section IV we will also employ the following result:

$$\begin{aligned} E_{\mathrm{G}} &= \arcsin\left[\sin P\sqrt{\cos^2\alpha_{\mathrm{L}} - \sin^2 E_{\mathrm{L}}} + \cos P\sin E_{\mathrm{L}}\right] \\ \alpha_{\mathrm{G}} &= \alpha_{\mathrm{L}} \\ A_{\mathrm{G}} &= \arcsin\left[\frac{\sin\alpha_{\mathrm{L}}}{\cos E_{\mathrm{G}}}\right] \end{aligned} \tag{7}$$

Observe that the transformations (5)-(7) are nonlinear, and that their nonlinearity grows with the antenna tilt and the angles. To illustrate the importance of this fact, consider a target whose base frame azimuth and elevation angles are A_{B} and E_{B}. Suppose that the array azimuth angle is ϕ_{a}. The GCS azimuth and elevation of the target are $A_{\mathrm{G}} = A_{\mathrm{B}} - \phi_{\mathrm{a}}$ and $E_{\mathrm{G}} = E_{\mathrm{B}}$. Using (5) and (6) one may obtain the LCS coordinates of the target as functions of the ϕ_{a}. Fig. 4 shows the resultant trajectories for a target at $A_{\mathrm{B}} = 0°$, $E_{\mathrm{B}} = 50°$, antenna tilt $P = 20°$, and $\phi_{\mathrm{a}} \in [-60°, 0°]$. Note that A_{L} is *not* a linear function of ϕ_{a} (although the difference from the linear approximation is indeed small in the case presented) nor it is simply equal to $-\phi_{\mathrm{a}}$. The pattern of LCS coordinates suggests that the nonlinearity and the interdependence of the transformations between LCS and GCS may complicate the estimation of target DoA, because an estimator of azimuth will require an estimate of target elevation and vice versa.

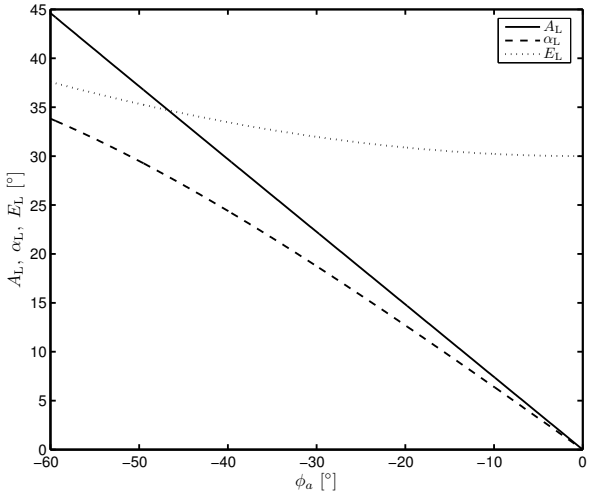

Figure 4. Typical behavior of LCS target coordinates as a function of antenna rotation angle.

IV. Proposed approach

A. Basic scheme

To be practically applicable in radar, a DoA estimator should, among others, have modest computational complexity, behave well at low signal to noise ratios, and exhibit good accuracy for small and high steering angles. To satisfy these requirements we propose a scheme that: 1. Avoids joint estimation of azimuth and elevation to keep its computational complexity low. 2. Employs coherent integration or processes entire data sequence to avoid ill behavior at low signal to noise ratio. 3. Accounts for the intrinsic coupling between coordinates.

Our solution that is best suited to situations where the beamwidth in the elevation plane is several times larger than in the azimuth plane. To illustrate, consider a planar array built on the square grid of sources (half-wavelength element spacing is assumed, $d = \lambda/2$). The dimensions of the array are $R = 16$ elements in the vertical axis (rows) and $C = 48$ elements in the horizonal axis (columns). Suppose that beams are formed by applying separate weights in the horizontal and the vertical planes,

$$\begin{aligned} \boldsymbol{w}_{\mathrm{H}} &= \left[w_{\mathrm{H},1}\ \ldots\ w_{\mathrm{H},C}\right]^{\mathrm{T}} \\ \boldsymbol{w}_{\mathrm{V}} &= \left[w_{\mathrm{V},1}\ \ldots\ w_{\mathrm{V},R}\right]^{\mathrm{T}}\ , \end{aligned}$$

computed as follows

$$\begin{aligned} w_{\mathrm{H},i} &= t_{\mathrm{H},i}e^{j\frac{2\pi d}{\lambda}c\sin(\phi_\alpha)} \qquad & c &= 1, 2, \ldots, C \\ w_{\mathrm{V},i} &= t_{\mathrm{V},i}e^{j\frac{2\pi d}{\lambda}r\sin(\phi_E)} \qquad & r &= 1, 2, \ldots, R \end{aligned}$$

where $t_{\mathrm{H},i}$ and $t_{\mathrm{V},i}$ are the horizontal/vertical taper functions, respectively, and ϕ_α, ϕ_E denote the beam steering angles. The resultant beampattern in the $(\alpha_{\mathrm{L}}, E_{\mathrm{L}})$ coordinate system can be computed from

$$B(\alpha_L, E_{\mathrm{L}}) \propto \left[\boldsymbol{w}_{\mathrm{V}}^{\mathrm{H}}\boldsymbol{a}_{\mathrm{V}}(E_{\mathrm{L}})\right]\left[\boldsymbol{w}_{\mathrm{H}}^{\mathrm{H}}\boldsymbol{a}_{\mathrm{H}}(\alpha_L)\right]\ ,$$

where

$$\begin{aligned} \boldsymbol{a}_{\mathrm{H}}(\alpha_L) &= \left[e^{j\frac{2\pi d}{\lambda}\sin(\alpha_L)}\ \ldots\ e^{j\frac{2\pi d}{\lambda}C\sin(\alpha_L)}\right]^{\mathrm{T}} \\ \boldsymbol{a}_{\mathrm{V}}(E_L) &= \left[e^{j\frac{2\pi d}{\lambda}\sin(E_L)}\ \ldots\ e^{j\frac{2\pi d}{\lambda}R\sin(E_L)}\right]^{\mathrm{T}}. \end{aligned}$$

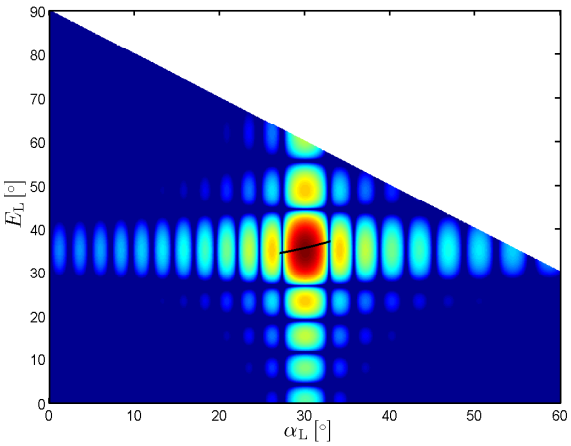

Figure 5. Typical trajectory of target coordinates $(\alpha_{\mathrm{L}}, E_{\mathrm{L}})$ during the scan of a mainlobe over a target, plotted using the thick black line. The coordinates in the white area do not satisfy the condition $\sin^2 \alpha_L + \sin^2 E_L \leq 1$.

Fig. 5 overlays the array beampattern with the trajectory of target LCS coordinates as the mainlobe of the beam sweeps over it due to the rotation of the array. The simulated target was placed at the base-frame azimuth and angle $A_{\mathrm{B}} = 0°$, $E_{\mathrm{B}} = 50°$. The beampattern was computed using $\phi_\alpha = 30°$, $\phi_E = 35°$ and the uniform taper. Finally, the array tilt was equal to $P = 20°$, and its rotation covered the angles $\phi_{\mathrm{a}} \in [-58°, -45°]$. Observe that, while both α_{L} and E_{L} of the target change during rotation, the change in E_{L} is much smaller, particularly if compared with the beamwidth in the corresponding plane. It follows that the degree of the signal nonstationarity is lower in the elevation plane, i.e., the use of the coherent integration of the sum and difference signals in this plane is more permissible than in the azimuth plane – particularly if one divides entire pulse trail into several shorter subtrails, which should reduce the bias of the subtrail estimates. The use of the same approach in the α plane is more difficult, because the subtrails should be shorter to achieve the same level of nonstationarity, which could result in an insufficient integration gain.

Interestingly, these factors are more pronounced at small steering angles, because in this case E_{L} becomes almost constant while the beamwidth in the azimuth plane decreases which decreases and increases the signal nonstationarity, respectively. Consequently, avoiding bias in the estimation of azimuth becomes easier at high steering angles, provided that one can properly take into account the beampattern deformations.

We summarize our approach below:

1) Collect N observations of sum and difference signals and divide them into K subtrails.
2) Find an initial estimate of the array azimuth that corresponds to the center of the beam passing over a target. The exact method of finding this estimate is not critical. To demonstrate this property, we deliberately use a very poor option of finding the array position $\phi_{\mathrm{a,max}}$ for which the highest magnitude of the sum was observed.
3) Compute the subtrail estimates of the elevation in LCS, preferably using coherently integrated (Doppler filtered) signals from each subtrail. Again, which method is used is not particularly important. To avoid complication, we will use the monopulse method. We denote these estimates $\hat{E}_{\mathrm{L},1},\ \hat{E}_{\mathrm{L},2},\ \ldots, \hat{E}_{\mathrm{L},K}$. Recall that these estimates have different expectations because of the array rotation (c.f. Fig. 5).
4) To compensate the drift of $\hat{E}_{\mathrm{L},1},\ \hat{E}_{\mathrm{L},2},\ \ldots, \hat{E}_{\mathrm{L},K}$ caused by the array rotation, one may employ the operation

$$\bar{E}_{\mathrm{L},k} = \hat{E}_{\mathrm{L},k} + \left.\frac{\partial E_{\mathrm{L}}}{\partial A_{\mathrm{G}}}\right|_{\alpha_{\mathrm{L}}=\phi_\alpha, E_{\mathrm{L}}=\hat{E}_{\mathrm{L},k}} (\bar{\phi}_{\mathrm{a},k} - \phi_{\mathrm{a,max}}) \tag{8}$$

where $\bar{\phi}_{\mathrm{a},k}$ is the averaged position of the array during the k-th subtrail and the derivative should be computed from (5)

$$\begin{aligned}\frac{\partial E_{\mathrm{L}}}{\partial A_{\mathrm{G}}} &= \frac{\partial}{\partial A_{\mathrm{G}}} \arcsin(\sin E_{\mathrm{L}}) \\ &= \frac{\sin A_{\mathrm{G}} \cos E_{\mathrm{G}} \sin P}{\cos E_{\mathrm{L}}} = \frac{\sin \alpha_{\mathrm{L}} \sin P}{\cos E_{\mathrm{L}}} .\end{aligned}$$

5) Compute the estimate of target elevation in the GCS $\bar{E}_{\mathrm{G}}$ using (7), α_{L} equal to the beam steering angle ϕ_α, and the averaged estimate of E_{L}

$$\bar{E}_{\mathrm{L}} = \sum_{k=1}^{K} w_k \bar{E}_{\mathrm{L},k} , \tag{9}$$

where w_k is a weight for the k-th subtrail that should be proportional to the SNR in this subtrail.
6) Estimate the target azimuth in the base frame coordinate system. To this end we will use the approximate stochastic maximum likelihood estimator proposed in [4], but application of other approaches, such as the one proposed in [3], is also possible. The estimator from [4] processes entire sequence of observations $\boldsymbol{y}_1,\ \boldsymbol{y}_2,\ \ldots, \boldsymbol{y}_N$, where each observation is a $M = 2$ element vector that consists of a pair of the sum and azimuth difference signals. The base-frame azimuth of the target is estimated by maximizing

$$\bar{A}_{\mathrm{B}} = \arg\max_{A_{\mathrm{B}}} \bar{l}(A_{\mathrm{B}}) , \tag{10}$$

where

$$\bar{l}(A_{\mathrm{B}}) = l(A_{\mathrm{B}}, \hat{\sigma}_v^2(\phi), \hat{\sigma}_{\mathrm{T}}^2(\phi))$$

is the compressed log-likelihood, obtained from

$$\begin{aligned} l(\phi, \sigma_v^2, \sigma_{\mathrm{T}}^2) &= C - \left[\sum_{n=0}^{N-1} \log\det \boldsymbol{R}_n + \boldsymbol{y}_n^{\mathrm{H}} \boldsymbol{R}_n^{-1} \boldsymbol{y}_n\right] \\ \boldsymbol{R}_n &= \sigma_v^2 \boldsymbol{I} + \sigma_T^2 \boldsymbol{b}(\Delta_n) \boldsymbol{b}^{\mathrm{H}}(\Delta_n) , \end{aligned} \tag{11}$$

and

$$\hat{\sigma}_v^2(\phi) = \frac{\sum_{n=0}^{N-1} \boldsymbol{y}_n^{\mathrm{H}} \boldsymbol{Q}_n(\phi) \boldsymbol{y}_n}{(M-1)N}$$
$$\hat{\sigma}_1^2(\phi) = \frac{\sum_{n=0}^{N-1} \boldsymbol{y}_n^{\mathrm{H}} \boldsymbol{P}_n(\phi) \boldsymbol{y}_n - N\hat{\sigma}_v^2(\phi)}{\sum_{n=0}^{N-1} \boldsymbol{b}^{\mathrm{H}}(\Delta_n)\boldsymbol{b}(\Delta_n)} \quad (12)$$

where

$$\boldsymbol{P}_n(\phi) = \frac{\boldsymbol{b}(\Delta_n)\boldsymbol{b}^{\mathrm{H}}(\Delta_n)}{\boldsymbol{b}^{\mathrm{H}}(\Delta_n)\boldsymbol{b}(\Delta_n)} \quad \boldsymbol{Q}_n(\phi) = \boldsymbol{I} - \boldsymbol{P}_n(\phi) \quad (13)$$

are the noise and the signal subspace projection matrices and $\boldsymbol{b}(\Delta_n)$ denotes the array response at the output of the beamformer to a wavefront impinging from the direction $(A_{\mathrm{G}}, E_{\mathrm{G}}) = (A_{\mathrm{B}} - \phi_{\mathrm{a},n}, \bar{E}_{\mathrm{G}})$, where $\phi_{\mathrm{a},n}$ is the azimuth of the array at the n-th observation . Note that, while the array response may be stored or computed in either GCS or LCS, in both cases the estimate $\bar{E}_{\mathrm{G}}$, obtained in the preceding step, will be required.

7) Replace $\phi_{\mathrm{a,max}}$ with an improved estimate obtained from $\bar{A}_{\mathrm{B}}$ and $\bar{E}_{\mathrm{G}}$. To this end, compute the deflection of the center of the beam at the elevation $\bar{E}_{\mathrm{G}}$ using the third formula in (7) and subtract this value from A_{B}

$$\phi_{\mathrm{a,max}} \leftarrow \phi_{\mathrm{a,max}} - \arcsin\left[\frac{\sin\phi_\alpha}{\cos\bar{E}_{\mathrm{G}}}\right] .$$

8) Repeat steps 2-6 until convergence.

B. Simplified scheme

Observe that, in the second and subsequent iterations of the proposed scheme, one can simplify steps 3-5 quite considerably. For example, step 3 does not need to be performed because the subtrail estimates $\hat{E}_{\mathrm{L},1}$, $\hat{E}_{\mathrm{L},2}$, $\ldots$, $\hat{E}_{\mathrm{L},K}$ are unchanged between iterations.

Moreover, one may expect the azimuth estimate found in the subsequent executions of step 6 are close to the azimuth found in the first iteration. We propose to exploit this fact by replacing the optimization performed in the second and subsequent iterations of step 6 with a simple iterative update

$$A_{\mathrm{G}} \leftarrow A_{\mathrm{G}} + \left.\frac{\partial A_{\mathrm{G}}}{\partial E_{\mathrm{G}}}\right|_{\alpha_{\mathrm{G}}=\phi_\alpha, E_{\mathrm{G}}=\bar{E}_{\mathrm{G}}} \Delta\bar{E}_{\mathrm{G}} , \quad (14)$$

where ΔE_{G} is the change of $\bar{E}_{\mathrm{G}}$ between the previous and current iteration and [c.f. (7)]

$$\frac{\partial A_{\mathrm{G}}}{\partial E_{\mathrm{G}}} = \frac{\partial}{\partial E_{\mathrm{G}}} \arcsin\left[\frac{\sin\alpha_{\mathrm{L}}}{\cos E_{\mathrm{G}}}\right] = \frac{\sin\alpha_{\mathrm{L}} \tan E_{\mathrm{G}}}{\sqrt{\cos^2 E_{\mathrm{G}} - \sin^2\alpha_{\mathrm{L}}}} .$$

V. Results of computer simulations

We compared the accuracy of the proposed scheme with three other approaches.

The first one is a straightforward monopulse that is carried out in the LCS separately for each of the N observations. Next, we convert such partial results to the GCS and add the position of the array to obtain N estimates of the base-frame azimuth and elevation. Finally, we average these estimates with weights that are proportional to the squared magnitude of the sum signal. One can expect this approach to work well for high SNRs but poorly for low SNR due to the fact that the partial estimates are worked out without any form of integration which causes a breakdown of their accuracy.

The second estimator is, again, the monopulse method, but this time we divide all observations into subtrails of equal length, and coherently integrate the signals in each subtrail. This estimator should behave better at low SNR, but might suffer from a bias that results from the process of integration.

The third solution is a stochastic maximum likelihood estimator that works directly in the two-dimensional space of base-frame azimuth and elevation. We implemented this estimator using (10)-(13), but this time the observation vector consisted of $M = 3$ elements, i.e., the sum, azimuth difference, and elevation difference signals. While this estimator can achieve very high accuracy, it has high computational complexity caused by the need to carry out the optimization in the two-dimensional space of parameters.

The implementation of the proposed estimator was based on its simplified variant, because our preliminary checks showed that the difference in accuracy from the basic version was marginal for steering angles up to $45°$, while the computation time – noticeably shorter. We also decided to use only two iterations, because additional ones did not bring significant improvement.

We simulated a radar using a planar array made of $R \times C = 24 \times 64$ sources on a square grid, tilted by $P = 20°$ and rotated between the angles $[-1.15°, +1.15°]$. The observations were taken every $0.1°$, which means that $N = 24$. The sum and two difference beams were formed using the uniform taper. Note that our simulation accounted for the two-way propagation.

Fig. 6 shows the dependence of mean-squared azimuth estimation errors of all estimators on signal to noise ratio for a target at $A_{\mathrm{B}} = 39°$, $E_{\mathrm{B}} = 4°$ and beam steered (in GCS) to $40°$ and $5°$, respectively. The results were obtained by performing 1000 Monte Carlo simulations for each value of SNR. Not unexpectedly, the two-dimensional stochastic maximum likelihood method performs best across all SNRs. The monopulse without coherent integration behaves well at high SNR, but its performance degrades at low SNR. The second variant of the monopulse works considerably better at low SNR. However, as SNR grows, its performance gradually lags behind and eventually saturates. The proposed approach in the basic variant compares favorably with all methods, in the sense that it shows excellent balance between the computational complexity and the accuracy, which almost matches the two-dimensional approach.

Fig. 7 shows analogous results for a target at $A_{\mathrm{B}} = 29°$, $E_{\mathrm{B}} = 29°$ and a beam steered to $30°$ and $30°$, and Fig. 8 – results for a target at $A_{\mathrm{B}} = 39°$, $E_{\mathrm{B}} = 29°$ and a beam at $40°$ and $30°$. In the first case one can make the same remarks as in the preceding paragraph. In the second case, even though strong broadening of the beam that results from steering in both planes makes the advantages of the proposed approach smaller, our scheme still exhibits top performance, particularly at low SNR. Eventually, at very high steering angles, the beam

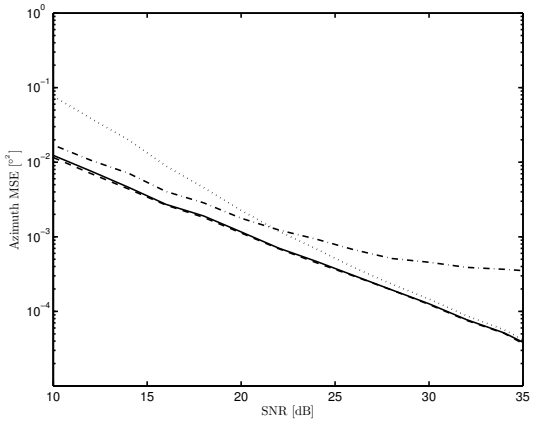

Figure 6. The comparison of mean-squared estimation errors of the azimuth as functions of signal to noise ratio for beam steered to 40° in GCS azimuth and 5° in GCS elevation. Dotted line – monopulse without coherent integration; dash-dotted line – monopulse with coherent integration; dashed line – two-dimensional stochastic maximum likelihood; solid line – proposed method.

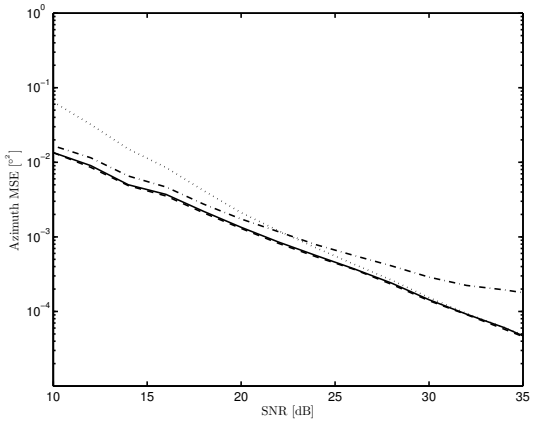

Figure 7. The comparison of mean-squared estimation errors of the azimuth as functions of signal to noise ratio for beam steered to 30° in GCS azimuth and 30° in GCS elevation. Dotted line – monopulse without coherent integration; dash-dotted line – monopulse with coherent integration; dashed line – two-dimensional stochastic maximum likelihood; solid line – proposed method.

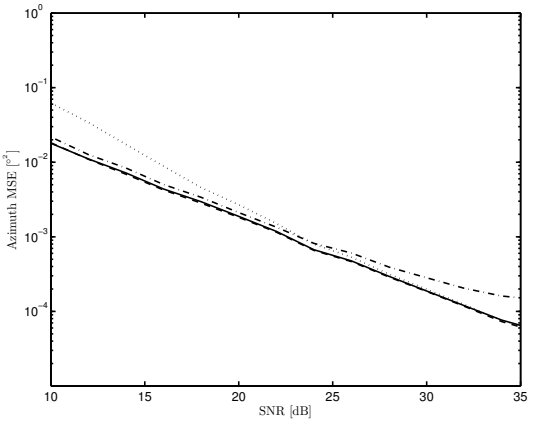

Figure 8. The comparison of mean-squared estimation errors of the azimuth as functions of signal to noise ratio for beam steered to 40° in GCS azimuth and 30° in GCS elevation. Dotted line – monopulse without coherent integration; dash-dotted line – monopulse with coherent integration; dashed line – two-dimensional stochastic maximum likelihood; solid line – proposed method.

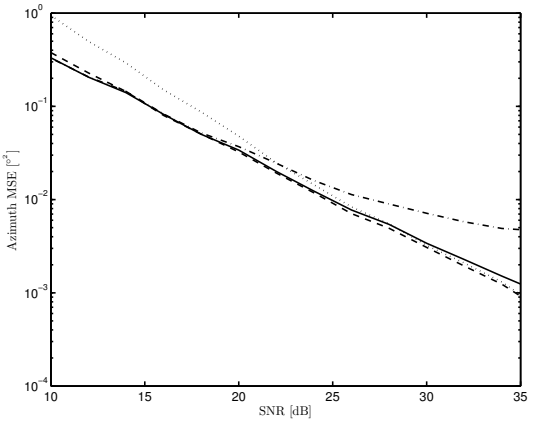

Figure 9. The comparison of mean-squared estimation errors of the azimuth as functions of signal to noise ratio for beam steered to 45° in GCS azimuth and 65° in GCS elevation with doubled antenna rotation speed and increased L. Dotted line – monopulse without coherent integration; dash-dotted line – monopulse with coherent integration; dashed line – two-dimensional stochastic maximum likelihood; solid line – proposed method.

broadens in the azimuth to such degree that the bias induced by the coherent integration becomes negligible compared to the variance under the conditions simulated and in the meaningful range of SNRs. One can make the bias a relevant component of the error by increasing the antenna rotation speed or increasing L. For example, Fig. 9 compares the accuracy of all methods for beam pointing to 45° in azimuth and 65° in elevation, target at $A_\mathrm{B} = 43^\circ$, $E_\mathrm{B} = 63^\circ$, antenna rotation speed increase twice and $L = 12$, in which case the benefits offered by the proposed approach are again clear. Note however, that at high SNR there occur first signs of the method's loss of efficiency, which are caused by the inaccuracy of the first order corrections in (8) and (14).

VI. Conclusions

We considered the problem of estimating azimuth and elevation coordinates using a tilted rotating-array radar system under high steering angles. We proposed an iterative approach that mitigates the need to estimate the two angles jointly, which reduces computational costs considerably. The method was compared with standard monopulse and a two-dimensional maximum likelihood estimator, and we found that it offers performance nearly equal to the latter.

References

[1] M. Skolnik, *Introduction to Radar Systems*. McGraw-Hill, 2002.
[2] D. K. Barton, *Radar System Analysis and Modeling*. Artech House, Inc., 2005.
[3] M. Greco, F. Gini, and A. Farina, "Joint use of Σ and Δ channels for multiple radar target DOA estimation," in *Proc. 2005 13th European Signal Processing Conference (EUSIPCO 2005)*, 2005.
[4] M. Meller, K. Stawiarski, and B. Pikacz, "Azimuth estimator for a rotating array radar with wide beam," *Proc. SPIE*, vol. 10715, pp. 10 715 – 10 715 – 5, 2018. [Online]. Available: https://doi.org/10.1117/12.2317865
[5] H. L. van Trees, K. L. Bell, and Z. Tian, *Detection, Estimation and Modulation Theory, Part I: Detection, Estimation, and Filtering Theory*. John Wiley & Sons, 2013.